Kinetics and Mass Transfer in the Hydrogenation of 2-((1-benzyl-1,2,3,6-tetrahydropyridin-4-yl)methylene)-5,6-dimethoxy--2,3-dihydroinden-1-one hydrochloride over Pt/C Catalyst

Z. Mastelić Samardžić,[a] Ž. Jelčić,[a] and S. Zrnčević[b,*]

[a]PLIVA Croatia LTD, R&D, Chemistry,
Prilaz Baruna Filipovića 25, Zagreb, Croatia

[b]University of Zagreb, Faculty of Chemical Engineering and Technology,
Zagreb, Croatia

doi: 10.15255/CABEQ.2013.1935

Original scientific paper
Received:
Accepted:

The liquid phase hydrogenation of 2-((1-benzyl-1,2,3,6-tetrahydropyridin-4-yl) methylene)-5,6-dimethoxy-2,3-dihydroinden-1-one hydrochloride **(1)** over a 5 % Pt/C industrial catalyst was studied experimentally in a batch slurry reactor using methanol as a solvent. The catalyst was characterized by the adsorption techniques for specific surface area and pore volume, and by XRD for crystallinity. To investigate the intrinsic kinetics of the reaction, the effect of temperature, catalyst loading, hydrogen partial pressure and **(1)** concentration on the initial rate of hydrogenation was studied. The analysis of initial rate data showed that the gas-liquid, liquid-solid, and intraparticle mass-transfer resistances were not significant. The reaction scheme of **(1)** hydrogenation was proposed for the kinetic modelling. Apparent rate constants for all hydrogenation steps were calculated using a first order kinetic approach resulting in good agreement between the experimentally obtained and predicted concentrations. From the temperature dependence of rate constants, the activation energies of various reaction steps were calculated. The averaged activation energy of these steps was found to be 31.1 kJ mol^{-1}.

Key words:
catalyst, hydrogenation, diffusion, kinetic modelling

Introduction

Selective catalytic hydrogenation of double and triple carbon-carbon bonds is one of the fundamental reactions for the synthesis of fine and industrial chemicals. This important area of catalytic chemistry has been the foundation for the development of numerous diverse, small- and large-scale commercial hydrogenation processes, which include synthesis of fine and specialty chemicals such as agrochemicals[1,2], flavours and fragrances[3–8], food additives[9–16] and pharmaceuticals[17–21].

The hydrogenation of 2-((1-benzyl-1,2,3,6-tetrahydropyridin-4-yl)methylene)-5,6-dimethoxy-2,3--dihydroinden-1-one hydrochloride **(1)** to 2-((1-benzylpiperidin-4-yl)methyl)-5,6-dimethoxy-2,3-dihydroinden-1-one hydrochloride **(4),** which is the last production step for the preparation of **(4),** is one such industrial important reaction. The reaction product is applied in the treatment of all kinds of senile dementia. In particular, it is useful for prevention and treatment of Alzheimer's disease by virtue of its acetyl cholinesterase inhibitory action[22].

There are many processes described mainly in patent literature[23–32] for producing **(4)** and its pharmaceutically acceptable salts. Complete chemo-selectivity is unlikely, because the starting compound **(1)** has more than one functionality susceptible to hydrogenation. There is a certain number of impurities that can be generated as side products of the reaction. The type of catalyst as well as reaction conditions for hydrogenation of **(1)** can significantly influence the yield of **(4)** and impurity profile. The yield of **(4)** can be low due to incomplete conversion of **(1)**. Alternatively, if **(1)** is completely consumed, the yield of **(4)** can be low due to competing side reactions where a number of by-products are generated, such as 5,6-dimethoxy-2-(piperidin-4-ylmethyl)-2,3-dihydroinden-1-one hydrochloride,1-benzyl-4-((5,6-dimethoxy-2,3-dihydro-1H-inden-2-yl)methyl)-piperidine hydrochloride, 2-((1-benzylpiperidin-4-yl)methyl)-5,6-dimethoxy-2,3-dihydro-1H-inden-1-ol hydrochloride and others. Recently, the authors presented a detailed study of the search for a catalyst that would meet requirements for high reaction selectivity and at the same time high activity, good stability, and possibility of the catalyst's reuse[33]. As expected in the hydrogenation of poly-unsaturated compound, different intermediates occur during the reaction. Based on experimental data, the reaction network given in Fig. 1 was derived for the hydrogenation of **(1)** to **(4)**. The re-

* Corresponding author: szrnce@fkit.hr

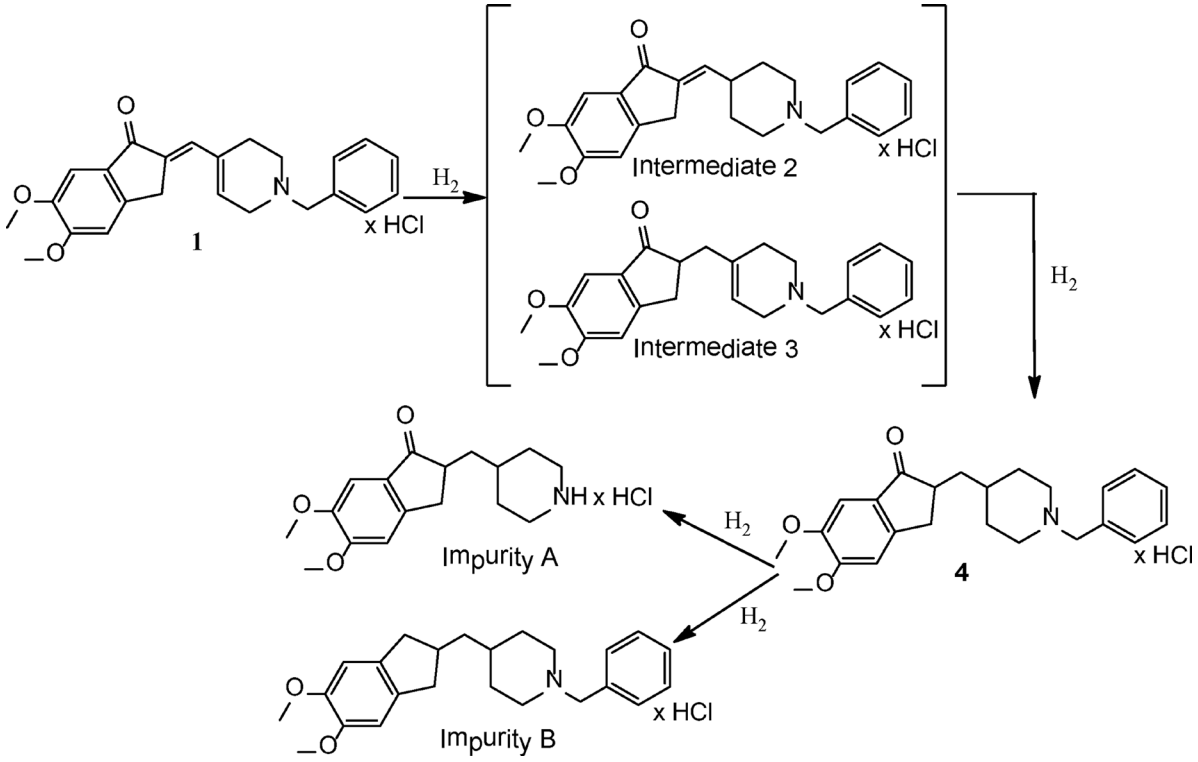

Fig. 1 – *Reaction network for* **(1)** *hydrogenation over Pt/C catalyst*

action pathway, involves the formation of **(4)** (with selectivity nearly 94 %), two intermediates **(2,3)** and two impurities **(A, B)** as the result of further hydrogenation of product **(4)**[33,34]. .

Liquid-phase hydrogenation over heterogeneous catalyst, in pharmaceutical production, is often performed in (semi)batch reactors, as they offer the possibility of a fast change of the production task, which is needed in this type of industry with production programs of a wide range of chemicals. Therefore, hydrogenation of **(1)** over 5 % Pt/C catalyst is carried out in mechanically agitated slurry reactors in which gas-liquid, liquid-solid and intraparticle diffusion resistances are likely to exist. For the purpose of kinetic study, it is important to ensure that the rate data are obtained under kinetically controlled regime or that the contribution of mass transfer is suitably incorporated or unimportant, under the reaction conditions studied, thereby ensuring a kinetically controlled regime. Considering the industrial significance of multiphase hydrogenation of **(1)** to **(4)** a detailed investigation on catalysis and kinetic modelling was undertaken in this work.

Experimental section

Materials

Compound **(1)** was produced by patent application WO/2007/015052 A1. The structure was confirmed by mass spectrum m/e 376 ($M+$, H^+); and by H^1 NMR (CF_3COOD, 600MHz) analysis: δ 3.30 (m, 1H), 3.55 (m, 1H), 3.70 (m, 1H), 4.20-4.36 (m, 2H), 4.30 (s,2H), 4.33 (s, 3H), 4.39 (s, 3H), 4.49 (m, 1H), 4.81 (m, 1H), 6.69 (s, 1H), 7.46 (s, 1H), 7.76 (s, 1H), 7.78-7.87 (m, 5H), 7.90 (s, 1H).

Commercial 5 % Pt/C catalyst (BASF, Italy) was used in hydrogenation experiments as received.

Catalyst characterisation

Textural characterisation of the catalyst samples was performed by means of nitrogen adsorption isotherms at 77 K using a Gemini 2380 Surface Area Analyzer (Micromeritics). Samples were outgassed at 423 K for 1 hour to remove adsorbed contaminants prior to the measurement. The BET specific surface area was calculated using the multipoint BET method on five points of the adsorption isotherm near monolayer coverage[35].

Crystalline structure of 5 % Pt/C catalyst was checked by X-ray diffraction analysis. XRD patterns were obtained with Philips PW 1830 diffractometer using Ni-filtered CuKα radiation operating at 40 kV and 30 mA. The patterns were recorded over $15^\circ < 2\theta < 70^\circ$ range using a step size of 0.02°.

2.3. Reaction procedure

The kinetic experiments were carried out in a commercial lab-scale 300 cm^3 stainless steel autoclave (*Parr Instrument Company, U.S.A.)*. The reactor was provided with the automatic temperature

control arrangement for sampling of liquids and variable agitation speeds. The details of the reactor set up were the same as described in our earlier paper[33]. In a typical hydrogenation experiment, predetermined quantities of **(1)**, catalyst and solvent methanol were charged into autoclave. The reactor was closed and the contents flushed three times with hydrogen. The reactor was then heated up to a desired temperature, pressurized with hydrogen to a desired level, and the reaction mixture was stirred with desired agitation speed. Pressure was maintained constant throughout the course of the reaction by supplying hydrogen from a reservoir vessel through a constant pressure-regulator valve. The moment when the desired pressure was achieved was assumed as the start (time = 0) of the reaction. The samples of reaction mixture were taken periodically from reactor, diluted with methanol and analyzed using high-pressure liquid chromatography. In the reaction mixture, the concentration of reactant **(1)**, product **(4)**, two intermediates **(2, 3)** and two impurities (**A, B)** were monitored. The ranges of operating conditions are given in Table 1.

Table 1 – *Range of parameters*

Catalyst loading, g dm^{-3}	0.57 – 2.86
Stirring speed, min^{-1}	100 – 500
H_2 partial pressure, MPa	0.2 – 3.0
(1) concentration, mol dm^{-3}	73 – 243
Temperature, K	298 – 318

Scale up of hydrogenation reaction on the industrial scale was conducted in *Pfaudler* batch reactor, V = 630 dm^3 (*Pfaudler*). The reactor was made of steel and equipped with a gas supply system (hydrogen and nitrogen). The reactor was heated by the reactor jacket and equipped with a sampling system.

The analysis of all samples was carried out using Agilent Technologies high-pressure liquid chromatography (model 1200) with DAD detector. The analytical conditions were as follows: Column & Packing: Phenomenex Gemini C18, 250 x 4,6mm (5 μm); Eluent A: Buffer NH_4OAc 10 mmol L^{-1}, pH = 6 diluted with acetonitrile in ratio of 2.7:1; Eluent B: Buffer NH_4OAc 10 mmol L^{-1}, pH = 4 diluted with acetonitrile in ratio of 0.54:1 Gradient: 0. min – 100 % A, 20. min – 0 % A Equilibration time: 20 min; Injection volume: 20 μL; Flow rate: 2.0 cm min^{-1}; Wavelength: 277 nm; Column temperature: 308 K; Autosampler temperature: 293 K.

NMR analysis was recorded on Bruker Avance DRX 600 NMR spectrometer operating at 600.1 and 150.9 MHz. CF_3COOD was used as a solvent.

Results and discussion

Catalyst characterization

The BET surface area and total pore volume of the supported Pt catalyst were 761 $m^2\ g^{-1}$ and 0.39 $cm^3\ g^{-1}$, respectively. In addition, the mean diameter of pores obtained from BET plot and pore size distribution was 2.04 nm.

The XRD pattern of Pt/C catalysts was collected in the range from 15° up to 70°. The catalyst exhibits a typical face-centred cubic (FCC) pattern, with the diffraction peaks at ~ 39°, 46° and 67°, assigned to the corresponding (111), (200) and (220), respectively (Figure 2). Several graphitic reflections are evident, the strongest of which is a sharp, symmetrical peak at 2θ = 26.3° assigned as the [002] plane of graphite[35,36]. The broad peaks in the XRD patterns indicate the small sizes of nanocrystals. The mean crystallite size derived from (220) plane XRD peak broadening, by applying the Scherrer's equation, was 7.6 nm.

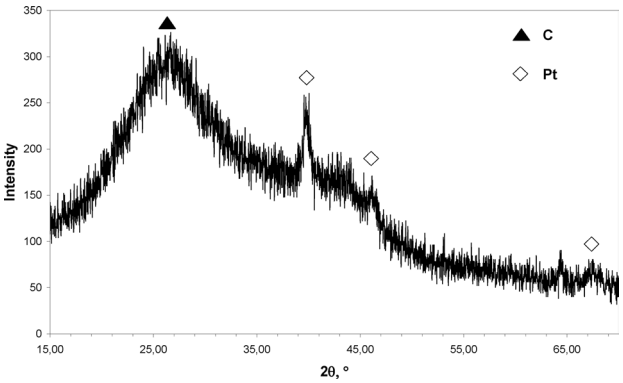

Fig. 2 – *X-ray diffraction pattern of 5 % Pt/C catalyst*

Kinetic studies

The hydrogenation experiments using 5 % Pt/C catalyst were performed to understand the overall kinetic of this reaction. For this purpose, experimental data were obtained by varying the operative conditions to observe the initial rate of hydrogenation as well as the integral concentration-time profiles. According to GLC and NMR data, the reaction pathway, as presented in Fig. 1, involves the formation of (**4)** (with selectivity nearly 94 %), two intermediates **(2, 3)** and two impurities **(A, B)** as a result of further hydrogenation of product (**4**). Impurity **(B)** is most difficult to eliminate by crystallization and re-crystallization processes[33]. At the end

of reaction, its content in the reaction mixture should not exceed $2.8 \cdot 10^{-4}$ mol dm^{-3}. Also, the content of impurity **(A)** should be below $1.0 \cdot 10^{-3}$ mol dm^{-3}. Since the formation of impurities A and B were below these values in all experiments, the reaction scheme presented in Fig. 1 was simplified as shown in Fig. 3.

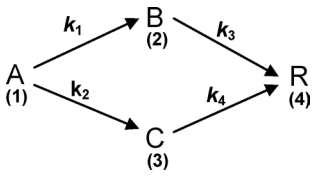

Fig. 3 – *Simplified reaction scheme for* **(1)** *hydrogenation over Pt/C catalyst*

The typical kinetic curves are presented in Fig. 4, demonstrating the dependence of the products composition *versus* reaction time at hydrogen pressure p_{H2} = 0.2 MPa and temperature 308 K over 5 % Pt/C catalyst.

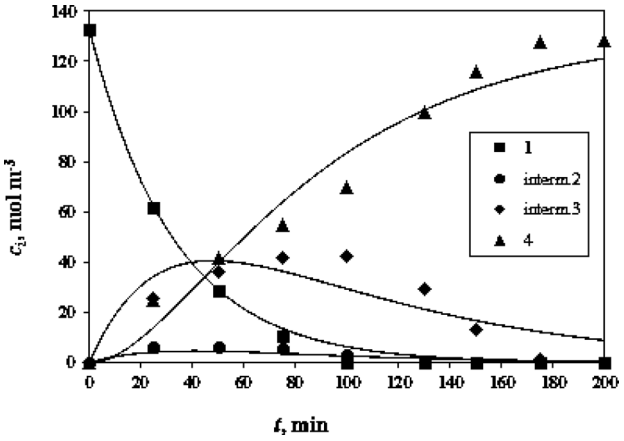

Fig. 4 – *Comparison of the model prediction (solid lines) with experimental data (symbols) of* **(1)** *hydrogenation over 5 % Pt/C (c_1= 0.14 mol dm^{-3}; p_{H2} = 0.2 MPa; T= 318 K; m_{cat} = 1.71 g dm^{-3}; V_{MeOH}= 0.175 dm^3,N = 400 min^{-1})*

3.2.1. Analysis of initial hydrogenation rates

The first approach to understanding the dependency of reaction rates on the individual reaction parameters as well as the significance of the mass transfer effect is the analysis of initial rate data. The separate effect of initial concentration of **(1),** hydrogen pressure and temperature on the initial rate data of hydrogenation of **(1)** was studied and the results are presented in Figs. 5-8.

The effect of concentration of **(1),** on the initial rate of hydrogenation is shown in Fig. 5. The rate of **(1)** hydrogenation is first order in the substrate at low concentration of substrate and approaches zero

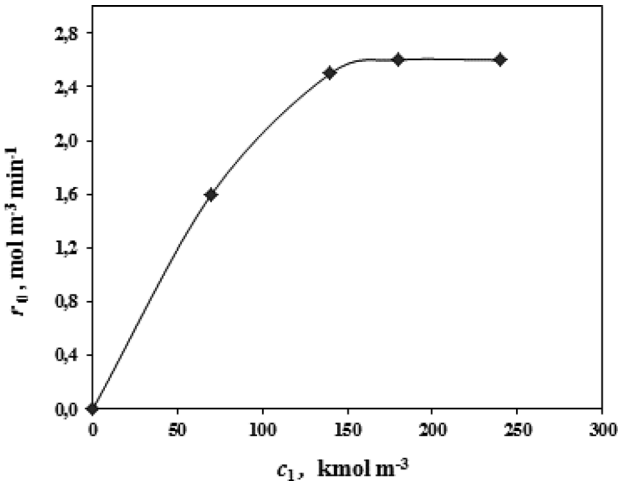

Fig. 5 – *Effect of* **(1)** *concentration on initial rate of hydrogenation (p_{H2} = 0.2 MPa; m_{cat} = 1.71 g dm^{-3}; T = 308 K; V_{MeOH}= 0.175 dm^3, N = 400 min^{-1})*

order at high concentrations of the substrate. These results indicate the non-linear behaviour of the rate of **(1)** hydrogenation, which is characteristic of a surface controlled reaction.

The initial reaction rates were also determined at various hydrogen pressures. Fig. 6 indicates nearly zero order dependence of the initial rate of reaction on hydrogen pressure, except at low partial pressures of hydrogen where the rate is directly proportional to the hydrogen pressure, and thus effectively exhibiting a first-order dependency on hydrogen.

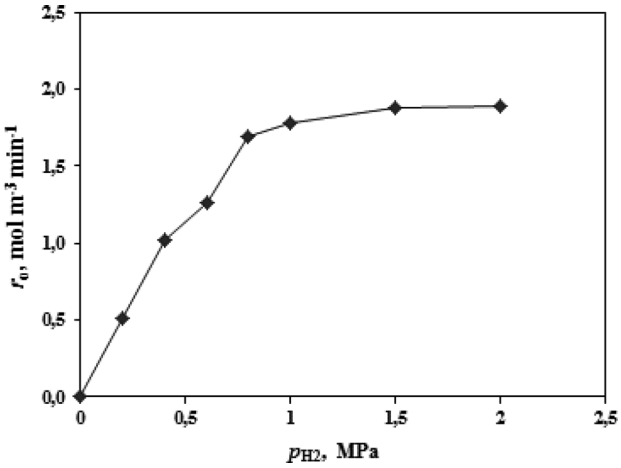

Fig. 6 – *Effect of hydrogen pressure on initial rate of hydrogenation (c_1= 0.14 mol dm^{-3}; m_{cat} = 1.71 g dm^{-3}; T = 308 K; V_{MeOH}= 0.175 dm^3, N = 400 min^{-1})*

The effect of temperature on the initial hydrogenation rate was studied in the range from 298 up to 318 K, at constant hydrogen pressure (0.2 MPa), and the results are presented in Fig. 7.

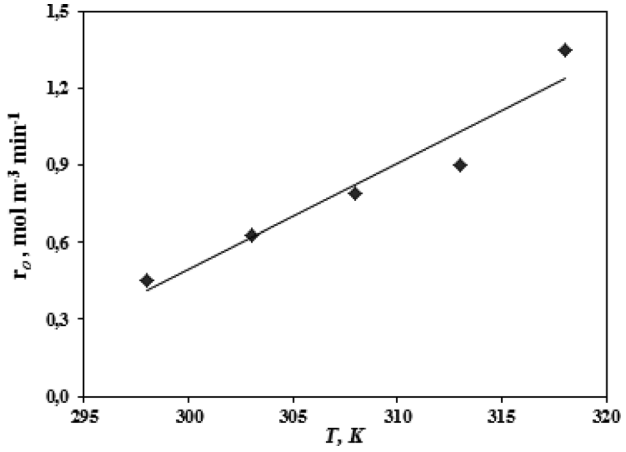

Fig. 7 – *Effect of temperature on initial reaction rate (c_1 = 0.14 mol dm^{-3}, V_{MeOH} = 0.175 dm^3, p_{H2} = 0.2 MPa, m_{cat} =1.71 g dm^{-3}, N = 400 min^{-1})*

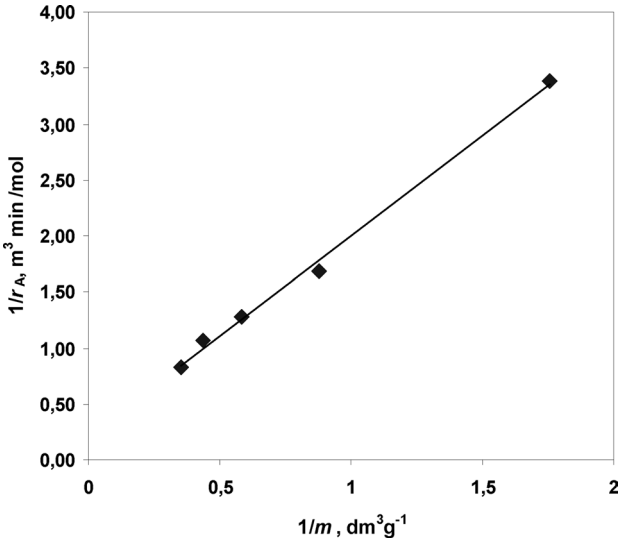

Fig. 8 – *Effect of inverse catalyst loading on the inverese of the rate of* **(1)** *hydrogenation (c_1= 0.14 mol dm^{-3}, p_{H2} = 0.2 MPa, T=308 K, V_{MeOH}= 0.175 dm^3, N= 400 min^{-1})*

As can be seen, the initial reaction rate varied linearly with temperature, which suggested that the reaction was intrinsically kinetically controlled and the activation energy values should be determined.

Influence of mass transfer

For the purpose of kinetic study, it is important to ensure that the rate data obtained were under conditions of chemical reaction control and that these data were not significantly influenced by mass transfer limitation. The initial rate data were analysed to check the significance of external (gas-liquid and liquid-solid) and internal mass transfer resistance.

The rate of reaction in a multiphase reactor for the case of first order reaction is given by the following equation proposed by Satterfield and Sherwood[37],

$$\frac{c_A^*}{r_A} = \frac{1}{k_{gl}a_g} + \frac{1}{m}\left[\frac{1}{k_{ls}a_s} + \frac{1}{k\,a_s\eta}\right] \qquad (1)$$

A plot of the inverse of the rate of reaction *versus* the inverse of catalyst mass density should give a straight line. This plot is given in Fig. 8 for experiments where the catalyst mass was varied from 0.57 to 2.86 g dm^{-3}.

The term $1/k_{ls}a_s$ of the plots in Fig. 8 represents a resistance associated with transport of hydrogen through bulk liquid. The term $1/k\,a_s\eta$ represents a resistance associated with the surface reaction. The intercept $1/k_{gl}a_g$ represents a resistance to gas adsorption across gas-liquid interface. From the intercept $k_{gl}a_g$ was 0.79 min^{-1}.

Further, in order to analyse the contribution of liquid-solid and intraparticle mass transfer effects on the rate of **(1)** hydrogenation, a knowledge of the liquid-solid mass transfer coefficient, k_s, effective diffusivity, D_e, external surface area of the catalyst particle, a_s, saturation solubility, c_A^* and the overall rate of hydrogenation, r_A are required.

The external surface area of the catalyst particle was calculated from the following equality, $a_s = m(6/d_p)(\rho_l/\rho_s)$ and was 260 $m^2_{cat}m_l^{-3}$. Solubility of hydrogen in methanol have been reported by Choudhary *et al.*[38] for relevant pressures and temperatures (293-328 K and 2.13 – 0.48 MPa) and a value of $H = 4.2\cdot10^{-2}$ MPa m^3 mol^{-1} was predicted from these data.

The effective diffusion coefficient, D_e is obtained from the molecular diffusion coefficient, D the catalyst particle porosity, e and tortuosity, t from the following expression

$$D_e = D\frac{\varepsilon}{\tau} \qquad (2)$$

The tortuosity and porosity of the catalyst were assumed to be 4 and 0.5, respectively[39].

The molecular diffusion coefficient for component dissolved in a solvent is calculated from Wilke and Chang[40] equation

$$D = 7{,}4\cdot10^{-12}\frac{T\sqrt{\chi M}}{\mu_l v^{0,6}} \qquad (3)$$

The calculated value of effective diffusivity along with other parameters is shown in Table 2.

The Weisz-Prater criterion[41,42] was used to determine diffusion resistance in porous Pt/C catalyst

$$\phi = \frac{r_A(d_p/2)^2}{c_{A,s}D_e} \qquad (4)$$

From Equation (4) using parameters given in Table 2, a value of Thiele modulus ϕ was calculated. A value for $\phi = 6.6 \cdot 10^{-4}$ indicates that the surface reaction rate is lower than the diffusion rate of a reactant within the pores of a catalyst[42] and the effectiveness factor ($\eta = \mathrm{tgh}\phi/\phi$) was 0.99.

Table 2 – *Values of different parameters used in evaluating the role of external and internal mass transfer resistance*

Catalyst/reactor data	
Catalyst particle diameter	$d_p = 2.5 \cdot 10^{-5}$ m
Catalyst particle density	$\rho_s = 1500$ kg m^{-3}
Tortuosity factor	$\tau = 4$
Particle porosity	$\varepsilon = 0.5$
Catalyst loading	$m = 1.75$ kg m^{-3}
Solvent	methanol
Liquid density	$\rho_l = 791.8$ kg m^{-3}
Liquid viscosity	$\mu_l = 5.9\ 10^{-3}$ kg m^{-1} min^{-1}
Stirring speed	$N = 400$ min^{-1}
Reactor volume	$V_R = 3 \cdot 10^{-4}$ m^3
Reaction conditions/parameters	
Reaction temperature	$T = 308$ K
H_2 pressure (constant)	$p_{H2} = 0.2$ MPa
Initial (**1**) concentration	$c_1 = 1.4 \cdot 10^2$ mol m^{-3}
Henry coefficient	$H = 4.2 \cdot 10^{-2}$ MPa m^3 mol^{-1}
Effective diffusion coefficient	$D_e = 2.4 \cdot 10^{-8}$ m^2 min^{-1}

The value of rate constant, k was calculated using equation (5)

$$r_A = k \eta a_s \frac{p_{H_2}}{H} \tag{5}$$

and it was $1.63 \cdot 10^{-3}$ min^{-1}, at hydrogen pressure of 0.2 MPa. From the slope of the curve presented in Fig. 5 and calculated values for k, a_s and h , the liquid-solid resistance was determined as $k_{ls} a_s = 0.137$ min^{-1}.

This analysis provides a rough indication that the external and internal mass-transfer resistances do not affect the rate of (**1**) hydrogenation i.e. hydrogenation rate is kinetically controlled. This conclusion was confirmed by the values of external effectiveness factors (gas-liquid) η_{gl} and (liquid-solid) η_{ls} which were 0.999 and 0.997 respectively.

Estimation of kinetics parameters

In order to describe the concentration profile of the species participating in the hydrogenation of **(1),** the simple estimating reaction scheme was proposed (Figure 3). According to the reaction scheme, first order kinetics with respect to the organic compounds was assumed for all hydrogenation steps

$$r_i = k c_{H_2} c_i = k' c_i \tag{6}$$

where the product $k c_{H2}$ was lumped pseudo-first order constant, because the hydrogen pressure in the gas phase was maintained constant in all experiments ($p_{H_2} = 0.2$ MPa), and because the solubility of hydrogen in the liquid phase was determined by its solubility in the solvent (as the concentration of substrate was low compared to the solvent concentration). The first order kinetic approach essentially assumes non-significant coverage of adsorbed reactant, which was justified by utilization of low **(1)** concentration.

The reaction kinetics can be described as follows. The disappearance of the reactant and the generation of the products can be calculated by the solution of the molar balances for the components in a batch reactor:

disappearance of reactant **(1)**

$$r_1 = -\left[\left(k_1 + k_2\right) c_1\right] \tag{7}$$

generation of intermediate **(2)**

$$r_2 = k_1 c_1 - k_3 c_2 \tag{8}$$

generation of intermediate **(3)**

$$r_3 = k_2 c_1 - k_4 c_2 \tag{9}$$

generation of product **(4)**

$$r_4 = k_3 c_2 + k_4 c_3 \tag{10}$$

The apparent rate constant was determined based on the simple kinetic models. The model parameters were estimated by minimising the objective function

$$RMSD = \sum_{k=1}^{k=4} \frac{1}{N} \sqrt{\sum_{i=1}^{i=N} \left[\left(\frac{c_{k(\mathrm{mod}),i} - c_{k(\exp),i}}{c_{k,\max}} \right)^2 \right]} \tag{7}$$

where $c_{k(\mathrm{mod}),i}$ is the calculated concentration of component i, $c_{k(\exp),i}$ is measured concentration of component i, n is number of samples, and k is number of independent measured variables. The rate parameters estimated and *RMSD* values are given in Table 3 when hydrogenation of **(1)** was performed at various temperatures.

Table 3 – *Estimated kinetic parameters for hydrogenation of* **(1)**

T, K	k_1	k_2	k_3	k_4	RMSD
298	0.00194	0.00952	0.00556	0.01163	0.00626
303	0.00213	0.01540	0.00714	0.01423	0.00561
308	0.00241	0.01974	0.01004	0.02102	0.00618
318	0.00318	0.02466	0.01605	0.02831	0.00648

Example of the fit is provided in Figures 4 and 9 (when the reaction was carried out in laboratory and industrial reactor) showing apparently good agreement between the experimentally measured and predicted concentrations. The experimental and the predicted concentration-time data were found to agree within 5–9 % error.

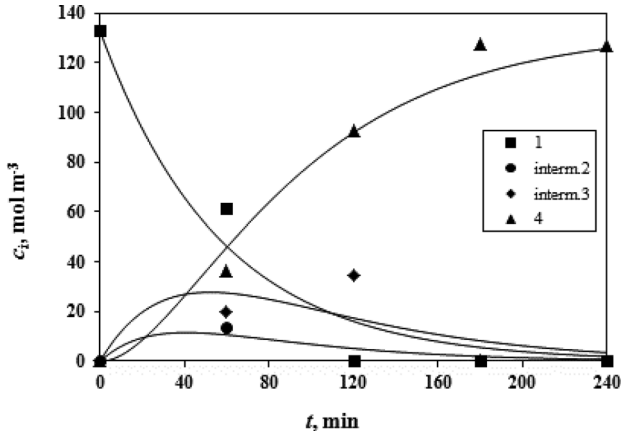

Fig. 9 – *Comparison of the model prediction (solid lines) with experimental data (symbols) of* **(1)** *hydrogenation over 5 % Pt/C in industrial reactor (c_1= 0.14 mol dm^{-3}, p_{H2} = 0.2 MPa, T = 308 K, m_{cat} = 1.71 g dm^{-3}, N = 400 min^{-1}, V_R=40 dm^3).*

The first order kinetic model allows estimation of the rate constants in **(1)** hydrogenation with high accuracy despite the apparent simplicity. The first order kinetic model is valid in the case of low surface coverage only and neglects differences in adsorption.

The observed energies of activation for formation of intermediates and product of reaction were determined from the Arrhenius plot shown in Fig. 10, in which the rate constants against the reciprocal of the temperature were plotted. The experiments were carried out in the temperature range 298 – 318 K at constant hydrogen pressure (0.2 MPa). From the temperature dependence of rate parameters, the activation energies of various reaction steps were calculated. These values of activation energies for steps, r_1, r_2, r_3 and r_4 are presented in Table 4.

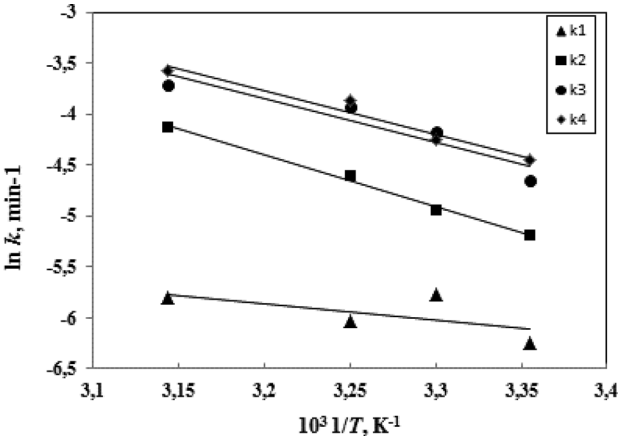

Fig. 10 – *Temperature dependence of rate constants*

Table 4 – *Activation energies for steps r_1, r_2, r_3 and r_4*

	Reaction	E_a, kJ mol^{-1}
r_1	A → B	40.8
r_2	B → R	34.3
r_3	A → C	14.4
r_4	C → R	34.7

Hydrogenation of reactant **(1)** to intermediate **(3)** (A ® B) is rate determining step deducing from high value for energies of activation, E_a. The hydrogenation of C=C double bond in the bridge of reactant **(1)** molecule is very quick (A ® C) with low value for E_a. Energies of activation for hydrogenation of both intermediates **(2)** and **(3)** to product **(4)** (B ® R, C ® R) are practically the same. The value of the averaged activation energy of these four reaction steps, 31.1 kJ mol^{-1}, is in agreement with those generally reported for the double bond hydrogenation reaction carried out in kinetic regime[18, 43–46].

Conclusion

The hydrogenation of 2-((1-benzyl-1,2,3,6-tetrahydropyridin-4-yl)methylene)-5,6-dimethoxy-2,3--dihydroinden-1-one hydrochloride **(1)** to 2-((1-benzylpiperidin-4-yl)methyl)-5,6-dimethoxy-2,3-dihydroinden-1-one hydrochloride **(4)** using a 5 % Pt/C catalyst was studied in a batch slurry reactor in a temperature range of 298 – 318 K using methanol as solvent. The influence of catalyst loading, hydrogen partial pressure, and reactant concentration on the hydrogenation rate was investigated. The analysis of initial rate data showed that the gas-liquid, liquid-solid, and intraparticle mass-transfer resistances were not significant. The reaction scheme of **(1)** hydrogenation was proposed for the kinetic modelling. Apparent rate constants of all hydroge-

nation steps were estimated by the first-order kinetic approach. Very good agreement between experimentally recorded concentrations and those predicted by the kinetic model was achieved. From the temperature dependence of rate constants, the activation energies of various reaction steps were calculated. The averaged activation energy of these steps, 31.1 kJ mol^{-1} is in agreement with that generally reported for the double bond hydrogenation reaction carried out in kinetic regime.

Nomenclature

c_A^* – saturation solubility of H_2, mol m^{-3}
c_{As} – surface concentration of A, mol m^{-3}
c_1 – concentration of reactant **(1)**, mol m^{-3}
c_2 – concentration of intermediate **(2)**, mol m^{-3}
c_3 – concentration of intermediate **(3)**, mol m^{-3}
c_4 – concentration of product **(4)**, mol m^{-3}
d_p – catalyst particle diameter, m
D – molecular diffusion coefficient, m^2 min^{-1}
D_e – effective diffusion coefficient, m^2 min^{-1}
E_a – activation energy, kJ mol^{-1}
H – Henry coefficient, MPa m^3 mol^{-1}
k_1- k_4 – reaction rate constant of respective steps, min^{-1}
$k_{gl}\,a_g$ – gas-liquid mass transfer coefficient, min^{-1}
$k_{ls}\,a_s$ – liquid-solid mass transfer coefficient, min^{-1}
m – catalyst loading, kg m^{-3}
M – molecular mass, kg mol^{-1}
N – stirring speed, min^{-1}
p_{H2} – hydrogen pressure, MPa
$r_1 - r_4$ – reaction rate of respective steps, mol m^{-3} min^{-1}
t – time, minutes
T – temperature, K
v – molar volume, mol m^{-3}

Greek letters

χ – association factor of solvent,–
ε – particle porosity, –
ϕ – Thiele modulus, –
η – effectiveness factor, –
μ_l – liquid dynamic viscosity, kg m^{-1} min^{-1}
ρ_l – liquid density, kg m^{-3}
τ – tortuosity factor, –

References

1. *Giornal, F., Pazenok, S., Rodefeld, L., Lui, N., Vors, J-P., Leroux, F.R.,* Synthesis of diversely fluorinated pyrazoles as novel active agrochemical ingredients**,** J. Fluorine Chem. **152** (2013) 2. http://dx.doi.org/10.1016/j.jfluchem.2012.11.008
2. *Spindler, F., Pugin, B., Blaser, H.U.,* Novel diphosphino-iridium catalyst for the enantioselective hydrogenation of N-arylketimines, Angew. Chem. Int. Ed. Engl. **29** (1990) 558. http://dx.doi.org/10.1002/anie.199005581
3. *Bønnemann, H., Brijoux, W., Schulze Tilling, A., Siepen, K.,* Application of heterogeneous colloid catalysts for the preparation of fine chemicalsTop. Catal. **4** (1997) 217. http://dx.doi.org/10.1023/A:1019152625358
4. *Kukula, P., Červenú, L.***,** Hydrogenation of (2 E,4 E)-hexadienol, J. Mol. Catal. A. **148** (1999) 245. http://dx.doi.org/10.1016/S1381-1169(99)00157-0
5. *Kluson, P., Kukula, P., Kyslingerova, E., Červenú, L.,* Hydrogenation of 2,4-hexadienoic acid methyl ester, React. Kinet. Catal. Lett. **59** (1996) 9. http://dx.doi.org/10.1007/BF02067985
6. *Chapuis, C., Jacoby, D.,* Catalysis in the preparation of fragrances and flavours, Applied Catalysis A. **221** (2001) 93. http://dx.doi.org/10.1016/S0926-860X(01)00798-0
7. *Kukula, P., Červenú, L.*, The kinetics of methyl sorbate hydrogenation, Appl. Catal. A **177** (1999) 79-84. http://dx.doi.org/10.1016/S0926-860X(98)00258-0
8. *Gryaznov, V., Serebryannikova, O.S., Serov, Y.M., Emilova, M.M., Karavanov, A.N., Mischenko, A.P., Orenkhova, N.V.,* Preparation and catalysis over palladium composite membranes, Appl. Catal. A 96 (1993) 15. http://dx.doi.org/10.1016/0926-860X(93)80003-9
9. *Ortiz-Cervantes, C., García, J.J.,* Hydrogenation of levulinic acid to g-valerolactone using ruthenium nanoparticles, Inorg. Chim. Acta 397 (2013) 124. http://dx.doi.org/10.1016/j.ica.2012.11.031
10. *Hsu, R.M., Diosady, L.L., Rubin, L.J.*, Catalytic Behaviour of Palladium in the Hydrogenation of Edible Oils J. Am. Oil Chem. Soc. **65** (1988) 323. http://dx.doi.org/10.1007/BF02663075
11. *Santacesaria, E., Parella, P., Di Serio, M., Borelli, G*., Role of mass transfer and kinetics in the hydrogenation of rapeseed oil on a supported palladium catalyst, Appl. Catal. A **116** (1994) 269. http://dx.doi.org/10.1016/0926-860X(94)80294-7
12. *Savchenko, V.I., Makaryan, I.A.,* Palladium for the production of pure margarine, Platinum Met. Rev. **43** (1999) 74.
13. *Isler, O., Montavon, M., Ruegg, R., Zeller, P*., Die technische Synthese von β-Carotin. Helv. Chim. Acta **39** (1956) 249. http://dx.doi.org/10.1002/hlca.19560390128
14. *Chalid, M., Broekhuis, A.A., Heeres, H.J.*, Experimental and kinetic modeling studies on the biphasic hydrogenation of levulinic acid to g-valerolactone using a homogeneous water-soluble Ru-(TPPTS) catalyst, J. Mol. Catal. A. 341 (2011) 14. http://dx.doi.org/10.1016/j.molcata.2011.04.004
15. *Lavielle, S., Bory, S., Moreau, B., Luche, M.J., Marquet, A.,* A total synthesis of biotin based on the stereoselective alkylation of sulfoxides, J. Am. Chem. Soc. **100** (1978) 1558. http://dx.doi.org/10.1021/ja00473a038
16. *Ruppert, A.M., Paryjczak, T*., Pt/ZrO_2/TiO_2 catalysts for selective hydrogenation of crotonaldehyde: Tuning the SMSI effect for optimum performance, Appl. Catal. A. 320 (2007) 80. http://dx.doi.org/10.1016/j.apcata.2006.12.019
17. *Vilella, I.M.J., de Miguel, S.R., Scelza, O.A.,* Pt, PtSn and PtGe catalysts supported on granular carbon for fine chemistry hydrogenation reactions, J. Mol. Catalysis A. 284 (2008) 161. http://dx.doi.org/10.1016/j.molcata.2008.01.017
18. *Peter, S., Datsevich, L., Jess, A*., Kinetics of catalytic hydrogenation of b-ionone and application of a presaturated

one-liquid flow reactor for the production of fine chemicals, Appl. Catalysis A. 286 (2005) 96. http://dx.doi.org/10.1016/j.apcata.2005.03.010

19. *Eugene, P., Rausser, R., Nussbaum, A.L., Gebert, W., Hershberg, E.B., Tolksdorf, S., Eisler, M., Perlman, P.L., Pechet, M.M.,* 16-Alkylated corticoids.II. 9a-fluoro-16a-methylprednisolone 21-acetate, J. Am. Chem. Soc. **80** (1958) 4431. http://dx.doi.org/10.1021/ja01549a086
20. *Taub,.D., Hoffsommer, R.D., Slates, H.L., Wendler, N.L.,* 16b-methyl cortical steroids, J. Am. Chem.Soc. **80** (1958) 4435. http://dx.doi.org/10.1021/ja01549a095
21. *Machado, R.M., Broekhuis, R.R., Nordquist, A.F., Roy, B.P., Carney, S.R.*, Applying monolith reactors for hydrogenations in the production of specialty chemicals-process and economic considerations, Catal. Today 105 (2005) 305. http://dx.doi.org/10.1016/j.cattod.2005.06.036
22. The American Society of Health- System Pharmacists, AHFS® Consumer Medication Information, 2010.
23. *Gutman, A., Shokolnik, E., Tishin, B., Nisnevich, G., Zaltzman, I.,* (Finetech Laboratories Ltd.), U.S. Patent No. 6492522, 10 Dec 2002.
24. *Lerman, O., Kaspi, J., Arad, O., Alnabari, M.,Sery. Y.*, (Chemagis Ltd.), U.S. Patent No. 6844440, 18 Jan 2005.
25. *Reddy, M.S., Eswaraiah, S., Thippannachar, M.V., Chandrashekar, E.R.R., Kumar, P.A., Kumar, K. N.,* (Dr. Reddy's Laboratories, Inc.), U.S. Patent No. 7148354, 24 June 2002.
26. *Iimura, Y.,* (Eisai Co., Ltd.), U.S. Patent No. 6252081, 26 July 2001.
27. *Yatendra, K., Mohan, P., Asok, N., Nitin, M.,* (Ranbaxy Lab Ltd), WO Patent No. 2004082685A1, 30 Sep 2004.
28. *Sugimoto, H., Ogura, H., Arai,Y., Limura, Y., Yamanishi, Y.,* Research and development of donepezil hydrochloride, a new type of acetylcholinesterase inhibitor, Jap. J. Pharmacology **89** (2002) 7. http://dx.doi.org/10.1254/jjp.89.7
29. *Niphade, N., Mali, A., Taub,.D., Hoffsommer, R.D., Slates, H.L., Wendler, N.L.,Jagtap, K., Ojha, R.C., Vankawala, P.J., Mathad, V.T.*, An improved and efficient process for the production of donepezil hydrochloride: Substitution of sodium hydroxide for *n*-butyl lithium via phase transfer catalysis, Org. Process Res. Dev. **12** (2008) 731. http://dx.doi.org/10.1021/op800066m
30. *Attanti, S., Yadla, V.*, (Torrent Pharmaceuticals Ltd),WO Patent No. 2008010235, 24 Jan 2008.
31. *Ashvin, K., Aggarwal, C., Vankatesran, S., Lalit, W.*, US Patent No. 20100113793 A1, 6 May 2010.
32. *Thippannachar, M.V., Chintaman, N.N., Jayndal, V.P., Chaturlal, M.A.,* (Megafine Pharma (P) Ltd.), Indian Patent Application no. 1073/MUM/2008, 27 Nov 2008.
33. *Mastelić Samardžić, Z., Zrnčević, S.,* Catalytic hydrogenation in process of 2-((1-benzylpiperidin-4-yl)methyl)-5,6--dimethoxy-2,3-dihydroinden-1-one hydrochloride synthesis: Catalyst screening and optimization of reaction conditions, Polish J.Chem.Tech. **14** (2012) 38.
34. *Jelčić, Ž., Mastelić Samardžić, Z., Zrnčević, S.*, Fractal analysis of catalyst surface morphologies on hydrogenation in process of 2-((1-benzylpiperidin-4-yl)methyl)-5,6-dimethoxy-2, 3-dihydroinden-1-one hydrochloride synthesis, Appl. Catal.A. **456** (2013) 30. http://dx.doi.org/10.1016/j.apcata.2013.02.011
35. *Wenzhen Li , Changhai Liang, Weijiang Zhou, Jieshan Qiu, Zhenhua, Gongquan Sun and Qin Xin,* Preparation and characterization of multiwall carbon nanotubes supported platinum for cathode catalysts of DMFCs, J. Phys. Chem. B, **107** (2003) 6292. http://dx.doi.org/10.1021/jp022505c
36. *Klett, J., Hardy, R., Romine, E., Wells, C., Burchell, T.,* High-thermal-conductivity, mesophase-pitch-derived carbon foams: effect of precursor on structure and properties Carbon **38** (2000) 953–973. http://dx.doi.org/10.1016/S0008-6223(99)00190-6
37. *Satterfield, C.D., Sherwood, T.K.,* The Role of Diffusion in Catalysis, Addison-Wesley, Reading, MA, 1963, pp. 43.
38. *Choudhary, V.R., Sane, M.G., Vadgaonkar, G.,* Solubility of hydrogen in methanol containing reaction species for hydrogenation of o-nitrophenol J.Chem.Eng.Data **32** (1986) 294. http://dx.doi.org/10.1021/je00045a011
39. *Satterfield, C.N.,* Heterogeneous Catalysis in Practice, McGraw-Hill Book Co., New York, 1980, pp. 336.
40. *Wilke, C.R., Chang, P.A.*, Correlation of diffusion coefficients in dilute solutions, A.I.Ch.E.J. **1** (1955) 264. http://dx.doi.org/10.1002/aic.690010222
41. *Weisz, P.B., Prater, C.D.,* Interpretation of measurements in experimental catalysis, Adv.Catal. **6** (1954) 143-196. http://dx.doi.org/10.1016/S0360-0564(08)60390-9
42. *Weisz, P.B.*, Diffusivity of porous particles. I. Measurements and significance for internal reaction velocities, Z. Phys.Chem. **11** (1957) 1. http://dx.doi.org/10.1524/zpch.1957.11.1_2.001
43. *Semikolenov, V.A., Ilyna, I.I., Simakova, I.L.,* Linalool synthesis from α-pinene: kinetic peculiarities of catalytic steps, Appl. Catal. A. 211 (2001) 91. http://dx.doi.org/10.1016/S0926-860X(00)00841-3
44. *Deliy, I.D., Smikova, I.L., Ravasio, N., Psaro, R.*, Catalytic behaviour of carbon supported platinum group metals in the hydrogenation and isomerization of methyl oleate, Appl. Catal.A. 357 (2009)170. http://dx.doi.org/10.1016/j.apcata.2009.01.026
45. *Mathew, S.P., Rajasekharam, M.V., Chaudhari, R.V.,* Hydrogenation of *p*-isobutyl acetophenone using a Ru/Al_2O_3 catalyst: reaction kinetics and modelling of a semi-batch slurry reactor, Catal. Today 49 (1999) 49. http://dx.doi.org/10.1016/S0920-5861(98)00407-6
46. *Breen, J.P., Burch, R., Gomez-Lopez, J., Gtiffin, K., Hayes, M.*, Steric effects in the selective hydrogenation of cinnamaldehyde to cinnamyl alcohol using an Ir/C catalyst, Appl.Catal.A. 268 (2004) 267. http://dx.doi.org/10.1016/j.apcata.2004.04.002